Clinical Whole-Brain R2* and Quantitative Susceptibility Maps at 3T -Reproducibility and Parameter Optimization Towards Millimetric 5min Scan

T Troalen, A Le Troter, S Confort-Gouny, P Vioux, C Costes, L Pini, J P Ranjeva, M Guye, Ludovic de Rochefort

Clinical Whole-Brain R2* and Quantitative Susceptibility Maps at 3T – Reproducibility and Parameter Optimization Towards Millimetric 5min Scan

T. Troalen[1], A. Le Troter[2], S. Confort-Gouny[2], P. Vioux[2], C. Costes[2], L. Pini[2], J.P. Ranjeva[2], M. Guye[2], L. de Rochefort[2]

1- Siemens Healthcare SAS, Saint-Denis, France
2- CRMBM UMR7339 CNRS Aix-Marseille Université, Marseille, France

Labels:

Brain, Susceptibility, Clinical Application, Data Processing,

Synopsis:

Advanced reconstruction techniques allow to jointly estimate R2* and QSM in the brain from multi gradient-recalled echo sequences. This work aims at comparing several protocols in terms of coil setup and acceleration factors using available product sequences and modern hardware. In addition, an automatic and standardized post-processing pipeline is proposed for clinical studies. We show that quantitative values do not differ in terms of head coil, repetition time and acceleration factor used, thus allowing for a millimetric whole-brain coverage within 5 minutes scan time.

Summary of Main Findings:

This work demonstrates the reproducibility in time, between systems and protocols for joint R2* and QSM in the brain in the same volunteer in clinical setups. The ability to reduce scan time without loss of sensitivity is shown, reaching a whole brain millimetric clinical protocol of 5min.

Introduction

Quantitative susceptibility mapping[1] (QSM) and R2* mapping techniques are now considered as quantitative biomarkers of iron, calcium and myelin[2,3] brain tissue content, with previously reported alterations in several neurological pathologies involving neurodegeneration, inflammation, oncology or trauma[1,4-14].

To facilitate clinical translation of QSM and to improve scan time efficiency, this study aims at comparing several protocols in terms of head coils, acceleration factors and repetition times. Reproducibility of the QSM data obtained on different MR scanners was also investigated. In a "travelling subject" setup, all the results were obtained from the same volunteer, with an automatic processing pipeline providing quantitative values in various brain regions.

Methods

Experiments were performed over 3.5 years on a healthy volunteer (37-y.o. at first pass) on different clinical 3T systems (MAGNETOM Verio, and MAGNETOM Vida, Siemens Healthcare, Erlangen, Germany) with body coil transmission and different coil-density receive head coils (32-channel head, 20-channel and 64-channel head/neck). The protocol included a 3D T1w anatomical reference (MPRAGE, ADNI) repeated on each scanner and for each coil used.

R2*/QSM acquisitions were all based on a millimetric spoiled multi-echo gradient-recalled echo (GRE) sequence with fixed echo times ranging from 4.22ms to 30.50ms. The original 10min protocol was taken from a clinical multicentric whole-brain T2* mapping protocol at 3T[15] standardized across hardware from several manufacturers, and consisting of the acquisition of six successive monopolar gradient echoes with a net GRAPPA acceleration factor of 3.

Relevant protocol parameters are reported in Table 1. Briefly, the original 10min protocol was repeated twice on the Verio system with three years interval between scans. Four months later, the same protocol was repeated on Vida system using the same 32Ch head coil, as well as the 20Ch and 64Ch head/neck coils. Next, the protocol was acquired with a reduced repetition time of 35ms instead of 54ms. The acceleration factor was then increased to 4 using a Caipirinha pattern in both phase encoding directions to finally achieve a 5min scan time compatible with clinical routine.

The reconstruction of R2* and QSM maps was done as in reference[16,17] using automatic Morphology Enabled Dipole Inversion[18,19]. On the Verio system, coil combination was performed using a specific reconstruction program using the first echo phase as a reference. On the Vida, the default phase reconstruction was used in the adaptive combined mode[20].

The automatic post-processing pipeline is reported in Figure 1 and consisted in several co-registration steps, label propagation from the MNI template and tissue segmentation using SPM12. The entire pipeline is described in the figure's legend.

Results

Representative R2* and QSM maps are shown in Figure 1. Contrast and image quality were qualitatively similar between all scans.

Regional values (mean and standard error of mean) of all extracted regions are reported in Figure 2 for the different protocols. Overall, both R2* and QSM values were in agreement between all scanners, coils and protocols, with an excepted higher R2* and QSM values in deep grey nuclei and especially in the pallidum[21].

Figure 3 highlights the reproducibility of the measurement across scanners, coils and sequence parameters. Apart from deep grey nuclei that are known to be heterogenous, the highest variations were found in the brain stem for R2* and between grey and white matters in the cerebellum for QSM.

Discussion

Extracted R2* and QSM values for the region of interest analysis are all in agreement between protocols and no difference could be observed.

As compared to the initial protocol optimized for Verio systems, we could reduce scan time below 5min for a full brain 1-mm isotropic coverage with a 64-channel coil, by shortening TR, and by using standard parallel imaging strategies. Although the multi-GRE sequence could be further accelerated by using compressed-sensing k-space trajectories and associated reconstructions algorithms, here the data acquisition needed for QSM is using product sequences that are available in standard clinical environments.

In the most recent system (Vida), we did not notice coil combination issues in the phase image generation suggesting that it is handled correctly using the default reconstruction program implemented by the manufacturer. Using a different coil setup did not affect the standard error of mean in the various regions suggesting that the variation might come from other sources (e.g. intrinsic error propagation in the R2* fitting and QSM inverse problem, or reproducibility of the segmentation).

We demonstrate insignificant temporal evolution in a volunteer for a period of more than three years, and yet on two different 3T systems providing confidence that on-going longitudinal clinical studies involving R2*/QSM can safely rely on these quantitative biomarkers. We have introduced here an analysis pipeline based on automatic brain region segmentation useful for quality analysis of acquisitions and QSM reconstruction pipelines, for protocol optimization and as an automatic diagnostic assistance tool for R2*/QSM.

Conclusion

This work demonstrates that the contrast mechanism in multi-GRE sequences is well preserved upon hardware equipment of the same manufacturer and that joint R2* and QSM measurement time can be reduced by a factor of two while preserving quantitative information using modern MR scanner with high-performance gradient and high-density receive coils. This may facilitate clinical implementation of R2* and QSM quantitative biomarkers protocols for brain characterization.

Acknowledgments

France Life Imaging, grant ANR-11-INBS-0006.

References

[1] L. de Rochefort *et al.*, « Quantitative susceptibility map reconstruction from MR phase data using bayesian regularization: validation and application to brain imaging », *Magn. Reson. Med.*, vol. 63, nº 1, p. 194-206, janv. 2010, doi: 10.1002/mrm.22187.

[2] Y. Wang *et al.*, « Clinical quantitative susceptibility mapping (QSM): Biometal imaging and its emerging roles in patient care », *J. Magn. Reson. Imaging JMRI*, vol. 46, nº 4, p. 951-971, 2017, doi: 10.1002/jmri.25693.

[3] S. Ropele et C. Langkammer, « Iron quantification with susceptibility », *NMR Biomed.*, vol. 30, nº 4, avr. 2017, doi: 10.1002/nbm.3534.

[4] S. K. Bandt *et al.*, « Clinical Integration of Quantitative Susceptibility Mapping Magnetic Resonance Imaging into Neurosurgical Practice », *World Neurosurg.*, vol. 122, p. e10-e19, févr. 2019, doi: 10.1016/j.wneu.2018.08.213.

[5] C. Langkammer *et al.*, « Quantitative Susceptibility Mapping in Parkinson's Disease », *PloS One*, vol. 11, nº 9, p. e0162460, 2016, doi: 10.1371/journal.pone.0162460.

[6] H.-G. Kim *et al.*, « Quantitative susceptibility mapping to evaluate the early stage of Alzheimer's disease », *NeuroImage Clin.*, vol. 16, p. 429-438, 2017, doi: 10.1016/j.nicl.2017.08.019.

[7] M. D. Santin *et al.*, « Reproducibility of R2 * and quantitative susceptibility mapping (QSM) reconstruction methods in the basal ganglia of healthy subjects », *NMR Biomed.*, vol. 30, nº 4, avr. 2017, doi: 10.1002/nbm.3491.

[8] A. Burgetova *et al.*, « Thalamic Iron Differentiates Primary-Progressive and Relapsing-Remitting Multiple Sclerosis », *AJNR Am. J. Neuroradiol.*, vol. 38, nº 6, p. 1079-1086, juin 2017, doi: 10.3174/ajnr.A5166.

[9] S. Ayton *et al.*, « Cerebral quantitative susceptibility mapping predicts amyloid-β-related cognitive decline », *Brain J. Neurol.*, vol. 140, nº 8, p. 2112-2119, août 2017, doi: 10.1093/brain/awx137.

[10] J. O'Callaghan *et al.*, « Tissue magnetic susceptibility mapping as a marker of tau pathology in Alzheimer's disease », *NeuroImage*, vol. 159, p. 334-345, oct. 2017, doi: 10.1016/j.neuroimage.2017.08.003.

[11] R. Cortese *et al.*, « Value of the central vein sign at 3T to differentiate MS from seropositive NMOSD », *Neurology*, mars 2018, doi: 10.1212/WNL.0000000000005256.

[12] N. Homayoon *et al.*, « Nigral iron deposition in common tremor disorders », *Mov. Disord. Off. J. Mov. Disord. Soc.*, vol. 34, nº 1, p. 129-132, 2019, doi: 10.1002/mds.27549.

[13] P. Maggi *et al.*, « Paramagnetic Rim Lesions are Specific to Multiple Sclerosis: An International Multicenter 3T MRI Study », *Ann. Neurol.*, vol. 88, nº 5, p. 1034-1042, 2020, doi: https://doi.org/10.1002/ana.25877.

[14] N. Pyatigorskaya *et al.*, « Iron Imaging as a Diagnostic Tool for Parkinson's Disease: A Systematic Review and Meta-Analysis », *Front. Neurol.*, vol. 11, p. 366, 2020, doi: 10.3389/fneur.2020.00366.

[15] D. Gay *et al.*, « A Standardised Clinical Multicentric Whole Brain T2* Mapping Protocol at 3T », ISMRM Singapore, 2016, p. 3305.

[16] L. de Rochefort *et al.*, « Clinical brain QSM acquisition and automated processing at 3T and 7T for routine use », ESMRMB Barcelona, 2017, p. 446, [En ligne]. Disponible sur: https://hal.archives-ouvertes.fr/hal-02559487.

[17] P. Spincemaille *et al.*, « Clinical Integration of Automated Processing for Brain Quantitative Susceptibility Mapping: Multi-Site Reproducibility and Single-Site Robustness », *J. Neuroimaging Off. J. Am. Soc. Neuroimaging*, vol. 29, nº 6, p. 689-698, 2019, doi: 10.1111/jon.12658.

[18] T. Liu *et al.*, « Morphology enabled dipole inversion (MEDI) from a single-angle acquisition: comparison with COSMOS in human brain imaging », *Magn. Reson. Med.*, vol. 66, nº 3, p. 777-783, sept. 2011, doi: 10.1002/mrm.22816.

[19] J. Liu *et al.*, « Morphology enabled dipole inversion for quantitative susceptibility mapping using structural consistency between the magnitude image and the susceptibility map », *NeuroImage*, vol. 59, nº 3, p. 2560-2568, févr. 2012, doi: 10.1016/j.neuroimage.2011.08.082.

[20] V. Jellus *et al*., « Adaptive Coil Combination Using a Body Coil Scan as Phase Reference », ISMRM Milan, 2014, p. 4406.

[21] W. Li *et al.*, « Differential Developmental Trajectories of Magnetic Susceptibility in Human Brain Gray and White Matter Over the Lifespan », Hum. Brain Mapp., vol. 35, p. 2698-2713, 2014, doi: 10.1002/hbm.22360

Table 1:

Main sequence parameters for the different protocols. Parameters that differ are highlighted in bold. Proposed comparison between experiments regarding R2* and QSM reproducibility for (1) system generations and receive head coils and (2) sequence parameters optimization (reduced repetition time of 35ms vs. 54ms and Caipi 4 vs. Grappa 3).

	Protocol	Common parameters	TR (ms)	Acceleration Factor	ACS	Coil	Base sequence	TA
1	**Verio** 32Ch Run 1&2	Matrix 256x256x160 Resolution 1mm iso Bandwidth 290 Hz/Px Flip Angle 15 deg Partial Fourier Off Echo Times 4.22 / 9.47 / 14.73 / 19.98 / 25.24 / 30.50	54	3 x 1	24 Separate	Head 32Ch	gre	10'
1	**Vida** 32Ch		54	3 x 1	24 Separate	**Head 32Ch**	gre	10'
1	Vida 20Ch		54	3 x 1	24 Separate	**Head/Neck 20Ch**	gre	10'
2	Vida 64Ch		**54**	3 x 1	24 Separate	**Head/Neck 64Ch**	gre	10'
2	Vida 64Ch TR35		**35**	**3 x 1**	**24 Separate**	Head/Neck 64Ch	**gre**	**6'30"**
2	Vida 64Ch Caïpi4		**35**	**2 x 2 (Caipi shift 1)**	**24x24 Separate**	Head/Neck 64Ch	**fl3d_vibe**	**4'53"**

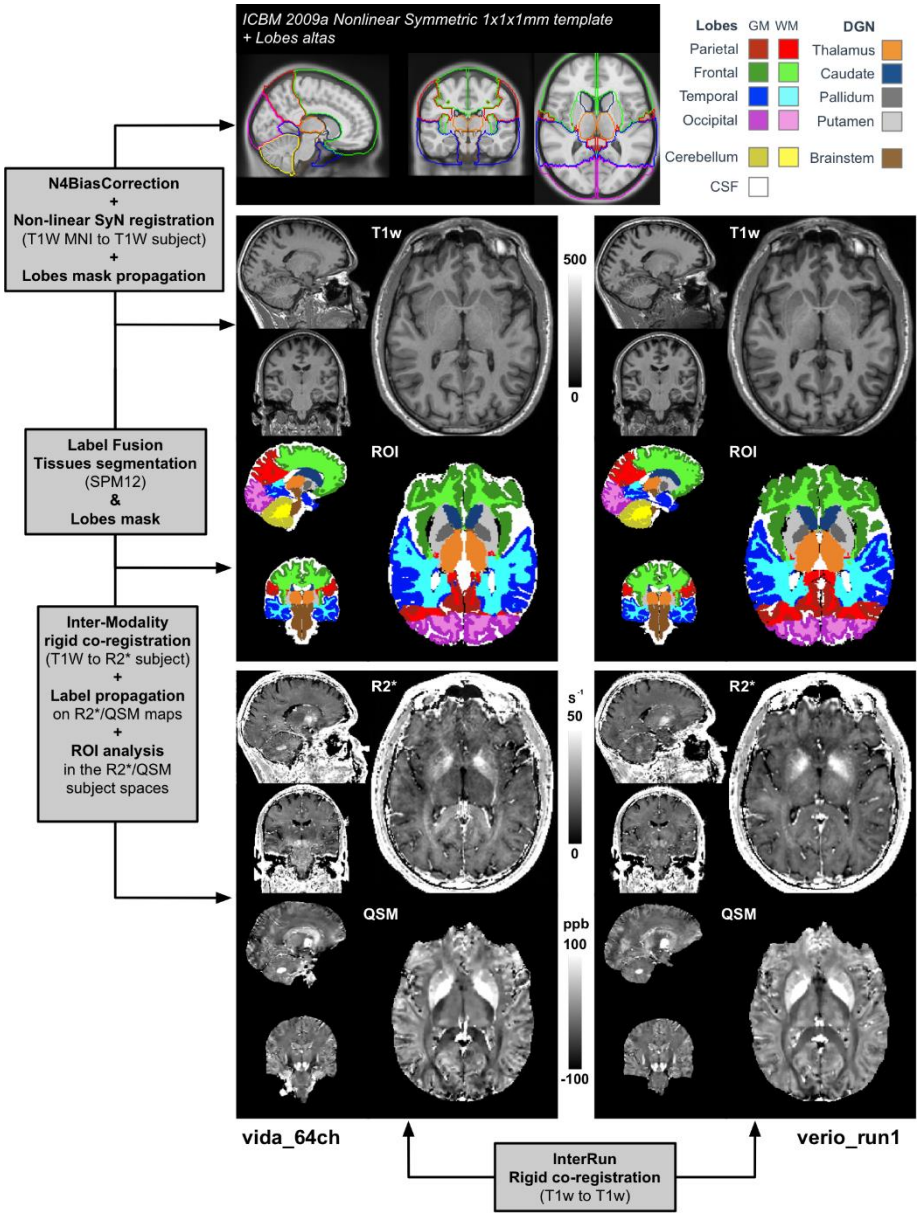

Figure 1: Automatic processing pipeline: The ICBM 2009a nonlinear symmetric MNI template was non-linearly registered to the subject's T1w space (using Vida_64Ch as reference).

Inter/Intra-run co-registrations were performed (T1wRef-to-T1w, as well as T1w-to-R2*). Tissue segmentation was achieved using SPM12 software using the default brain probability maps. Labels were propagated to R2*/QSM space and restricted to WM/GM tissue types. WM/GM lobes and cerebellum were extracted, as well as four deep grey nuclei and the brainstem prior ROI analysis on the quantitative maps.

Figure 2: Regional values (mean (top) and standard error of mean (bottom)) of the different scans in all regions of interest. Regional values are reported against ROI volumes to ensure a proper segmentation reproducibility among all acquisitions.

Apart from deep grey nuclei that are known to be heterogenous, the highest variations were found in the brainstem for R2* and between GM and WM in the cerebellum for QSM. This could be explained by the position of these regions with respect to the coil geometry (i.e. close to the neck) and potential CSF contamination (CSF volume variation).

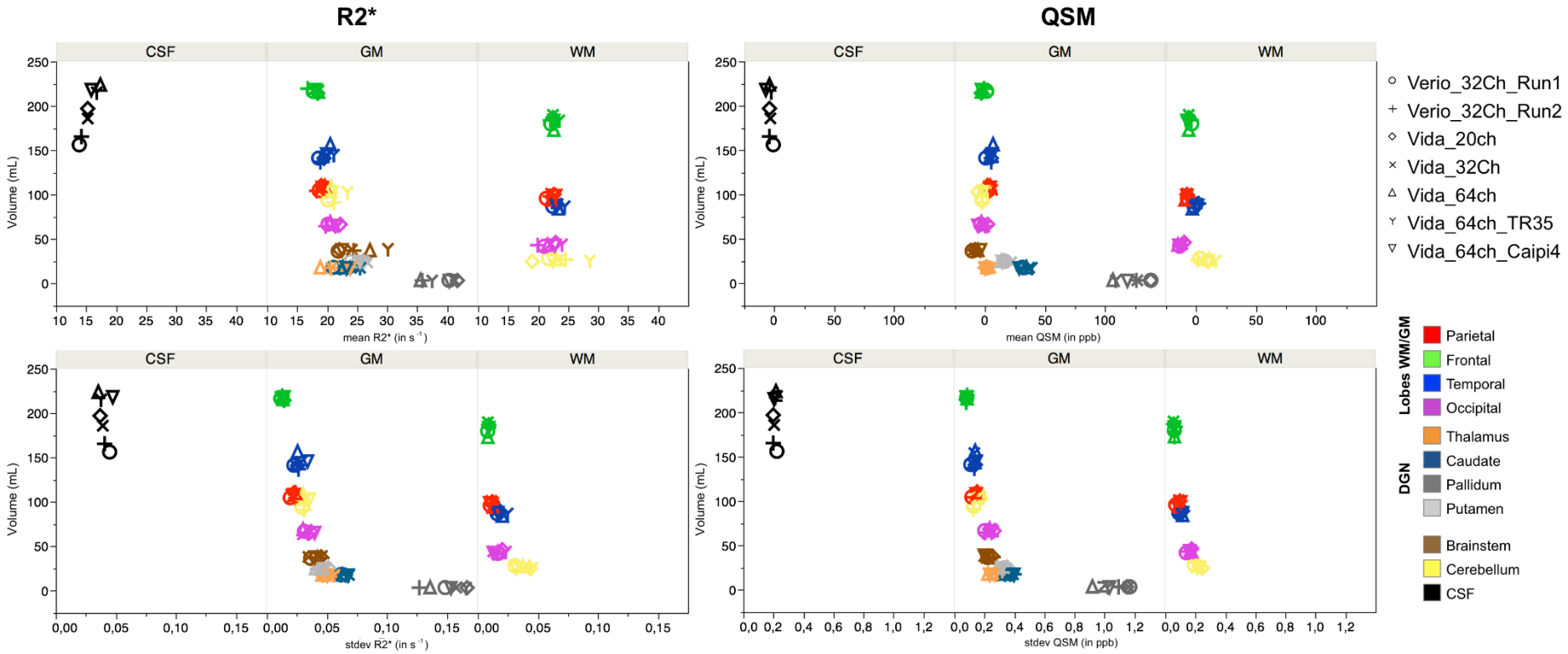

Figure 3:

Reproducibility across MR system types (Verio and Vida), receive head coils (20, 32 and 64 channels) and sequence parameters. Note that the measured variability on the Vida with different head coils was not different than the intra-run metric variations on the Verio system. The signal drop caused by the increased acceleration factor from 3 to 4 was not reflected in the R2* and QSM estimations, with values in the same range as the other protocols. The central table reports mean and standard deviation per segmented region across all measurements.

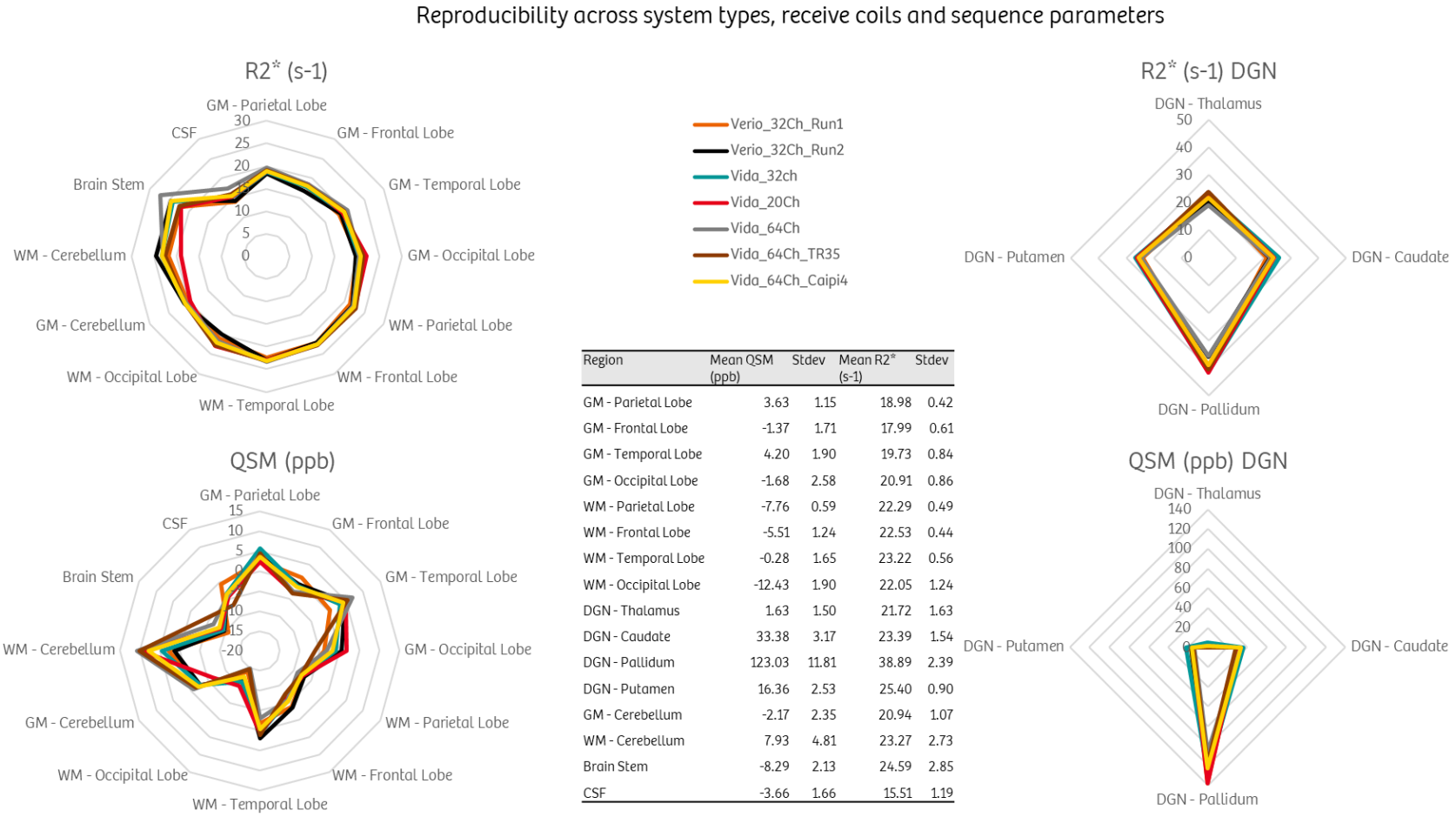

Region	Mean QSM (ppb)	Stdev	Mean R2* (s-1)	Stdev
GM - Parietal Lobe	3.63	1.15	18.98	0.42
GM - Frontal Lobe	-1.37	1.71	17.99	0.61
GM - Temporal Lobe	4.20	1.90	19.73	0.84
GM - Occipital Lobe	-1.68	2.58	20.91	0.86
WM - Parietal Lobe	-7.76	0.59	22.29	0.49
WM - Frontal Lobe	-5.51	1.24	22.53	0.44
WM - Temporal Lobe	-0.28	1.65	23.22	0.56
WM - Occipital Lobe	-12.43	1.90	22.05	1.24
DGN - Thalamus	1.63	1.50	21.72	1.63
DGN - Caudate	33.38	3.17	23.39	1.54
DGN - Pallidum	123.03	11.81	38.89	2.39
DGN - Putamen	16.36	2.53	25.40	0.90
GM - Cerebellum	-2.17	2.35	20.94	1.07
WM - Cerebellum	7.93	4.81	23.27	2.73
Brain Stem	-8.29	2.13	24.59	2.85
CSF	-3.66	1.66	15.51	1.19